



SRTTU

Journal of Computational and Applied Research  
in Mechanical Engineering

jcarme.sru.ac.ir

JCARME

ISSN: 2228-7922

## Research paper

## Investigation of the injection characteristics effect on the performance of diesel engine using annular injector

Rasool Esmaelnadjad<sup>a,\*</sup> and Navid Farrokhi<sup>b</sup>

<sup>a</sup>Mianeh technical and engineering faculty, University of Tabriz, Mianeh, Iran

<sup>b</sup>Department of Mechanical Engineering, Parand Branch, Islamic Azad University, Parand, Iran

### Article info:

#### Article history:

Received: 00/00/0000

Accepted: 00/00/0000

Revised: 00/00/0000

Online: 00/00/0000

#### Keywords:

Annular injector,  
Injection pressure,  
Injection duration,  
Engine performance,  
Specific fuel  
consumption.

#### \*Corresponding author:

[rasool\\_ra@tabrizu.ac.ir](mailto:rasool_ra@tabrizu.ac.ir)

### Abstract

Increasing the power and improving the performance of diesel engines is always considered by diesel engine manufacturers. Changing the geometry of the injector outlet orifice has major impact on fuel-air mixing and combustion. In the current study, geometry of the injector orifice is changed from circular to annular cross-section, and the effect of different injection pressures on diesel engine performance is investigated. All numerical simulations are performed by using AVL Fire code. The results show that the annular injector improves combustion and engine performance by forming better fuel distribution. Fuel injection pressure affects the performance of the annular injector in terms of droplets distribution and breakup. At low injection pressures, due to the long injection duration, most of the fuel energy release occurs after top dead center (TDC). Therefore, the engine performance is improved, and the combustion chamber temperature and pressure are limited. However, at high injection pressures, less combustion occurs after TDC. By changing the injector geometry to the injector with annular cross-section orifice, the maximum reduction in SFC value is for case P5 and injection durations 10 degrees, which is decreased by 21.4%. In the studied cases, the maximum power increase was 15% for a 2.5% increase of fuel at injection pressure of 100MPa. While NO pollutant increased slightly by changing the type of injector at different injection pressures, the soot produced at the beginning of the combustion process is well oxidized before the end of the work phase, and its amount reached less than  $2e-6$ .

### 1. Introduction

Combustion will be ideal when each fuel molecule is in the gas phase, and enough oxygen molecules are next to the fuel molecules during the chemical reaction. In this case, the

combustion process will be complete. The combustion mechanism inside the combustion chamber of diesel engines is of both non-premixed flame and diffusion flame. This means that when fuel is injected into the

combustion chamber, part of the fuel evaporates rapidly, and mixes with the air, and combustion inside the combustion chamber begins with the mixed fuels. The resulting flame at this stage is of the pre-mixed type. Afterwards, and with simultaneous fuel injection, the combustion mechanism changes from premixed flame to diffusion flame, and combustion continues. The role of injector type, injection duration and injection pressure in improving the performance of both combustion mechanisms in diesel engines is very important [1, 2].

Diameter of the initial droplets is also a very important parameter in how the fuel spray is formed. Smaller diameter of the droplets, leads to better formation of the primary and secondary droplets, which makes the droplets to be more uniform. To reduce the diameter of the droplets (considering the constant mass of the inlet fuel), one of the best solutions is to use multi-hole injectors, which in addition to reducing the diameter of the inlet droplets, causes a uniform distribution of fuel in the combustion chamber.

The use of this type of injectors causes better mixing of fuel and air, and also expands the area of the flame front inside the combustion chamber, which results in better diffusion of air into the flame front during combustion. This reduces the amount of pollutants produced. Although these types of injectors distribute the fuel spray evenly inside the cylinder compared to single-hole injectors, there are poor and rich areas of fuel in the spray of this type of injectors. Many numerical and experimental works have been conducted in this field [3-6].

One of the technologies to solve this problem is the use of micron-sized group holes. The purpose of using nozzles with very small and close holes is to improve the evaporation process of the fuel, without damaging the penetration length of the injector, through the two sprays collision. These types of injectors have also reduced soot and NO formation in diesel engines, and improved their performance [7-10].

Diameter of the initial droplets affects the length of the spray. Large diameters increase the penetration length, and impact of the droplets on the piston crown. When fuel droplets impact to the combustion chamber, the fuel distribution in the combustion chamber and mixing with the air is weakened. This reduces

the amount of air diffusion into the fuel spray, and increases the soot. The optimal state for designing the combustion process is a state in which both the amount of fuel spray evaporation and the penetration length are optimal. Therefore, in diesel engines, the fuel atomization process strongly affects combustion and emissions.

Number of the injector holes has special effect on performance and amount of diffusion because both parameters have important impact on the spray parameters such as droplet size and penetration length and thus the combustion process [11-15].

Initial shape of the inlet fuel flow is effective in creating the initial distortion and breakup of the droplets. Therefore, the use of non-circular orifice sections has also been considered by injector researchers. First, square, triangular and rectangular sections with low injection pressure were investigated [16, 17]. In order to use these injectors in diesel fuel injection, very high injection pressures were also investigated. Their results show that flat injectors have better injection angle [18].

Injectors with circular cross-section orifices are used in burners, as well as, agricultural, and pharmaceutical industries. So far, various shapes and sizes of orifices have been presented. The injection pressure is not so high in the injectors used in these industries. In this form of injectors, the outlet angle of the fluid can be adjusted using the needle tip at the outlet. Diameter of the droplets is also controlled using the ring thickness and the spray pressure. The outlet ring diameter is also used to control the fluid outlet flow [19]. The use of this type of injectors with very high injection pressure was investigated by Migliaccio et al. [20]. Based on their results, the spray from the annular cross-section injector has high injection angle and low penetration length, which can be used to inject large amount of fuel in a short time. The use of this type of injectors in gasoline engines has also been considered by researchers in the recent years [21-23].

Spray pressure is very effective in fuel flow rate, and how fuel droplets break. By increasing the injection pressure, velocity of the droplets entering the combustion chamber increases, and two phenomena cause faster breakup of the fuel droplets. The first phenomenon is related to the

movement of fuel inside the injector orifice. By increasing the velocity inside the orifice, effects of the boundary layer and the shear stress applied to the fuel cause more turbulence and more rotation of the fuel droplets when leaving the injector [24].

The second phenomenon is related to movement of the fuel inside the combustion chamber. The faster the fuel droplets enter the combustion chamber, the higher the probability of fuel droplets breaking (due to contact with air inside the combustion chamber) [25, 26]. Therefore, spray pressure is a very effective parameter in engine performance and production of pollutants [27-29].

Injection duration affects fuel-air mixing, combustion, air diffusion into the flame front, thermodynamic efficiency and temperature and pressure inside the combustion chamber. The effect of this parameter varies according to the type of fuel, the type of injector and the characteristics of the engine combustion chamber [30-33].

In the present work, it is tried to improve the fuel-air mixture in both combustion mechanisms by changing the type of injector, injection duration and injection pressure. In fact, using these three variables, it is supposed to increase the mixing percentage in the initial phase of spraying by evaporating the fuel faster. Also in the second phase of combustion (diffusion flame) there would be enough opportunity and space for fuel to diffuse into the flame.

The injector used has an outlet orifice with an annular cross-section. The thickness of the outlet ring is very small compared to the diameter of circular cross-section injectors, which causes smaller droplets to enter the combustion chamber with a larger injection angle, resulting in rapid breakup of the fuel droplets, rapid evaporation and their uniform distribution. Injection pressure and duration are effective in how the flame front moves. In the current study, the effects of the three mentioned variables have been investigated using computational fluid dynamics method with simulation in Fire software.

## 2. Methodology

Due to the fact that the annular injector outlet is in the form of a sheet, a sheet model is used to simulate the behavior of the spray inside the

cylinder. This represents a quasi-experimental model for the primary break-up of the injector outlet sheet. This model is used to determine the initial conditions of the spray such as sheet thickness, break-up velocity and length. Fig.1 shows the model schematic.

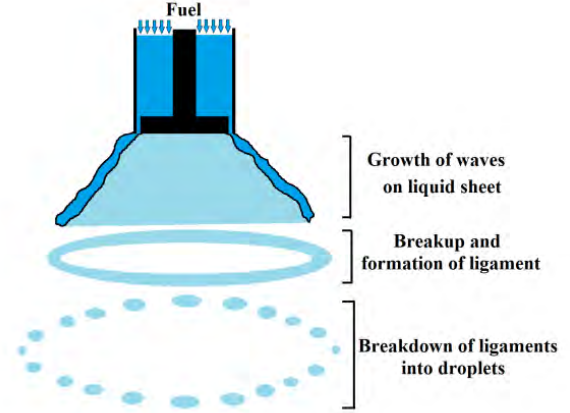


Fig. 1. Sheet breakup model.

In the mentioned model, fluid film thickness is calculated as [34]:

$$h = \left[ \frac{A \cdot 12 \cdot m_i \cdot \mu_1 \cdot (1+X)}{\pi \cdot \rho_f \cdot d_{out} \Delta p \cdot (1-X)^2} \right]^{0.5} \quad (1)$$

$$X = \frac{(d_{out} - 2 \cdot h)^2}{d_{out}^2} \quad (2)$$

Since  $h$ ,  $x$  are found from Eqs. (1 and 2), an iterative method is used to calculate the thickness.

The  $K_V$  velocity coefficient is defined as follows:

$$K_V = \frac{v}{(2 \cdot \Delta p / \rho)^{0.5}} \quad (3)$$

where  $K_V$  is calculated as:

$$K_V = \frac{C_3}{\cos \theta} \cdot \left( \frac{(1-X)}{1+X} \right)^{0.5} \quad (4)$$

The Clark-Dukowicz relationship is used to calculate the break-up length of the fluid sheet [35]:

$$B_L = B \cdot \left[ \frac{\rho_l \cdot \sigma \cdot \ln \left( \frac{\eta}{\eta_0} \right) \cdot h \cdot \cos \theta}{\rho_g^2 \cdot V_{rel}^2} \right]^{0.5} \quad (5)$$

On the flame front, which is a turbulent flow, reactants (fuel and oxidizer) have the same turbulence intensity that is different from the turbulence intensity of combustion reaction products. According to the turbulent combustion model, chemical reactions have much shorter time scale than the time scale of the turbulence transportation process. It can be assumed that the rate of combustion is

determined by the rate of mixing or collision of eddies including reactants and hot products at molecular scale. Therefore, the average reaction rate is expressed as [36]:

$$S_{fu} = \bar{\rho} \bar{r} = \frac{c_{fu}}{\tau_r} \bar{\rho} \cdot \min \left( \bar{y}_{fu}, \frac{\bar{y}_{ox}}{S}, \frac{c_{pr} \bar{y}_{pr}}{1+S} \right) \quad (6)$$

The soot model used in this study is based on Hiroyasu polluting pattern [37]. In this model, two physical and chemical processes are used to demonstrate the event of oxidation. Particle formation and surface growth are functions of fuel in a certain place of the combustion chamber and the concentration of soot core in that area, respectively. In this model, oxidized soot and the resulting soot are modeled:

$$\frac{dM_{soot}}{dt} = \frac{dM_{form}}{dt} - \frac{dM_{oxide}}{dt} \quad (7)$$

Soot formation is calculated as follows:

$$\frac{dM_{form}}{dt} = A_f M_{fv} P^{0.5} \exp \left( -\frac{E_f}{RT} \right) \quad (8)$$

The soot oxidation rate is calculated according to the following equation:

$$\frac{dM_{oxide}}{dt} = \frac{6MW_c}{\rho_s D_s} M_s R_{tot} \quad (9)$$

Reduction rate of the mixture is determined by the rate of dissolution and the rate of the local turbulent kinetic energy. Nitrogen oxide pattern used in Fire commercial code is the Clark-Dukowicz model [38]. This pattern is highly temperature dependent, and is produced by the reaction of nitrogen and oxygen at high temperatures. The concentration of nitrogen oxide has little effect on the flow, and the reaction time of nitrogen oxide is longer than the time interval intended for the mixing process and the combustion. Therefore, the calculations related to nitrogen oxide formation can be separated from the calculations for the main reaction. In this model, the multistage chemical reduction based on the partial equilibrium of the preliminary reactions is as follows:



The following general reaction is obtained by multiplying the right and left sides of the above equation:



Hence, the nitrogen oxide formation rate is extracted according to the following:

$$\frac{d[NO]}{dt} = 2k_f [N_2][O_2] \quad (12)$$

The reaction rate is also derived from the following relation [38]:

$$k_f = \frac{a}{\sqrt{T}} \exp \left( -\frac{E_a}{RT} \right) \quad (13)$$

### 3. Modeling

Investigation of annular injector behavior under different upstream and downstream conditions is considered. For this purpose, the flow inside the injector must be simulated. Fig. 2 shows the geometry of fuel inside the annular injector. The thickness of the injector outlet ring is 0.02 mm, which has an orifice length of 0.5 mm, ring diameter of 2 mm and nozzle outlet with a cone angle of 10°.

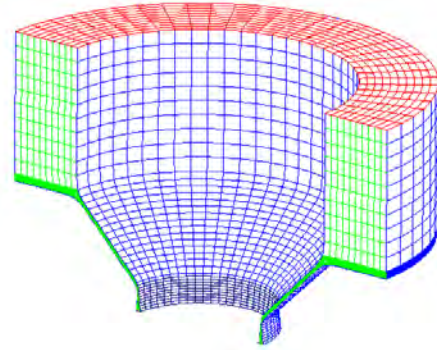


**Fig. 2.** Geometry of fuel volume inside the injector.

The main specifications and operating conditions of the engine used in the current research are given in Table 1. Geometry of the used engine is the same as that of the Kubota 3300 engine, which is a four-stroke direct injection diesel engine with natural aspiration.

**Table 1.** Engine geometry.

|                   |      |
|-------------------|------|
| Cylinders number  | 4    |
| Bore (mm)         | 98   |
| Stroke (mm)       | 110  |
| Engine volume (L) | 3.32 |

In this study, 5 different injection pressures are used to inject fuel into the combustion chamber. The studied cases are given in Table 2. Every injection pressure comes along with three different injection durations. Longer injection duration has been used at low injection pressures, while shorter injection duration has been used at high injection pressures. The selection of these injection durations was based on the production capacity of the Kubota



engine. The start time of fuel injection in all the studied cases is 20 degrees bTDC.

**Table 2.** The studied cases.

| Case number | Injection pressure (MPa) | Flow rate (kg/s) | Injection duration (deg) |
|-------------|--------------------------|------------------|--------------------------|
| P1          | 40                       | 0.0055           | 22                       |
|             |                          |                  | 20                       |
|             |                          |                  | 18                       |
| P2          | 60                       | 0.007            | 20                       |
|             |                          |                  | 18                       |
|             |                          |                  | 16                       |
| P3          | 80                       | 0.0083           | 18                       |
|             |                          |                  | 16                       |
|             |                          |                  | 14                       |
| P4          | 100                      | 0.0092           | 16                       |
|             |                          |                  | 14                       |
|             |                          |                  | 12                       |
| P5          | 120                      | 0.0101           | 14                       |
|             |                          |                  | 12                       |
|             |                          |                  | 10                       |

AVL Fire commercial code was used for conducting 3D simulations, and the quarter geometry of the engine cylinder chamber was modeled and meshed. Fig. 3 shows the combustion chamber in both the TDC and BDC states. The type of piston crown used in the present study has been changed because while the circular cross-section injector injects fuel to the central region of the cylinder, annular injectors (used in the Kubota 3300 engine) sprays it at a certain angle to the cylinder walls. In the present work, the type of fuel and its temperature are constant. The estimated values for the fuel characteristics are given in Table 3. The internal conditions of the cylinder at the beginning of compression stroke are considered to be constant in all cases. The specifications are given in Table 4.

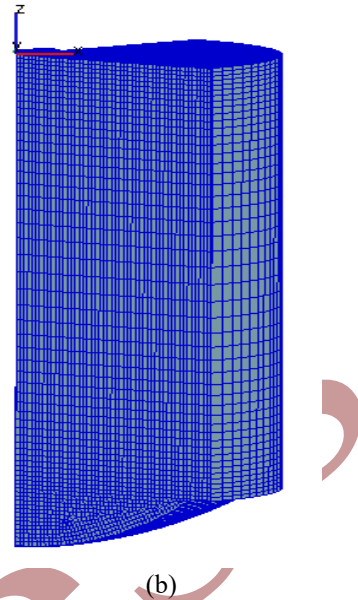
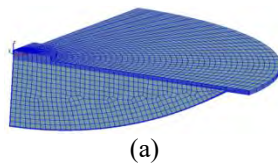


**Fig. 3.** Combustion chamber at: (a) top dead center and (b) bottom dead center.

**Table 3.** Fuel characteristics.

| Density (kg/m <sup>3</sup> ) | Dynamic viscosity (Ns/m <sup>2</sup> ) | Temperature (K) |
|------------------------------|--|-----------------|
| 830                          | 0.00214                                | 293.15          |

**Table 4.** Condition of the cylinder at the beginning of the compression.

| Temperature (K) | Pressure (kPa) | Air density (kg/m <sup>3</sup> ) |
|-----------------|----------------|----------------------------------|
| 293             | 100            | 1.21                             |

**4. Grid independency**

Results of the solution should be independent of the number of the cells. For this purpose, by producing meshes with different cell numbers, the suitable cell number is selected. The basis of the grid independency is the results of cylinder internal pressure. Four different computational cell numbers were used. The pressure changes versus the crank angle for different cell numbers are shown in Fig. 4.

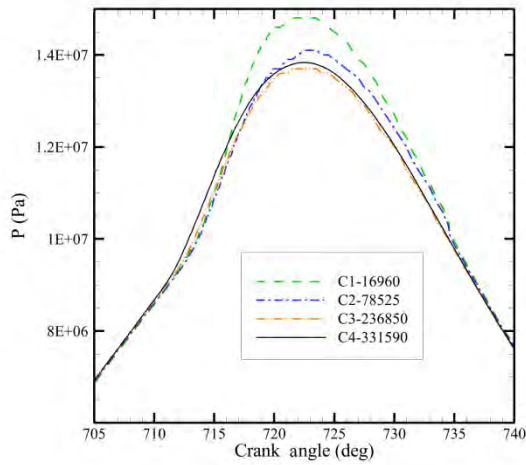


**Fig. 4.** Pressure variations for different grids.

As can be seen, the pressure changes from the third cell number are very small. Therefore, meshing with cell number 236850 is used.

**5. Numerical method validation**

Before changing the type of injector in the Kubota engine from a conventional multi-hole injector to an annular injector, the combustion performance of the Kubota 3300 engine was simulated with its conventional injector. The engine was tested and numerically simulated at 2600rpm and a compression ratio of 22.6. Fuel spraying starts 20° bTDC and is 36 mg per spray. The results obtained for power, SFC and production of NO and soot pollutants were compared and validated with the experimental results of Hassan et al. [39].

The results of numerical simulation demonstrate acceptable agreement with their results. The results of numerical analysis and experimental tests are given in Table 5 for engine performance and in Figs. 5, 6 for produced pollutants.

**Table 5.** Comparison of the numerical and experimental results.

| Parameter    | Numerical value | Experimental value |
|--------------|-----------------|--------------------|
| Power (kW)   | 48.88           | 47.9               |
| SFC (kg/kWh) | 0.244           | 0.237              |

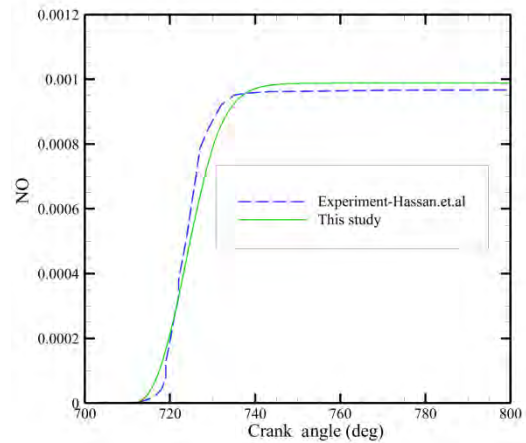


**Fig. 5.** NO emissions validation.

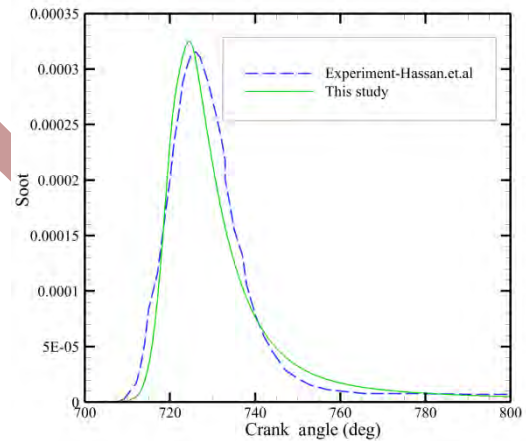


**Fig. 6.** Soot pollutant validation.

**6. Results and discussion**

In the present study, the effects of using annular cross-section injector and different injection pressures on diesel engine performance were investigated. The numerical results of the research are presented in the form of hydrodynamic behavior, fuel spray development pattern and engine performance parameters, as well as the amount of emissions. Fuel type, compression ratio, the starting angle of injection and geometry of the Kubota 3300 engine were constant.

The nozzle type was changed from a typical six-hole orifice to an orifice with annular cross-section, and the piston crown shape was changed accordingly. The mass entering the combustion chamber in one cycle for 5 different

injection pressures for the annular injector along with the amount of fuel injection in the Kubota engine is shown in Fig. 7. In the first case (P1) due to the low injection pressure (40MPa) three injection durations of 22, 20 and 18 degrees were used, while in the fifth case (P5) due to the high injection pressure (120MPa) three injection durations of 14, 12 and 10 degrees were used. At each injection pressure, three injection durations were used. Thus, the fuel inlet mass (fuel consumption) must increase gradually with increasing pressure, but as shown in Fig. 7, the upward trend is to the third injection pressure (P3), and afterwards, the inlet mass has decreased. The reason for this is the boundary layer separation and slight evaporation of fuel in the injector orifice.

The separation was also predictable because with increasing injection pressure, the velocity of fuel inside the injector orifice is increased, and a partial separation occurs in the orifice path. For the cases P1 and P2 and injection durations 20 degrees, compared to the Kubota 3300 engine, injected fuel mass is decreased by 23.9% and 4.17%, respectively. The maximum reduction is for case P1 and injection durations 18 degrees, which is decreased by 31.4%.

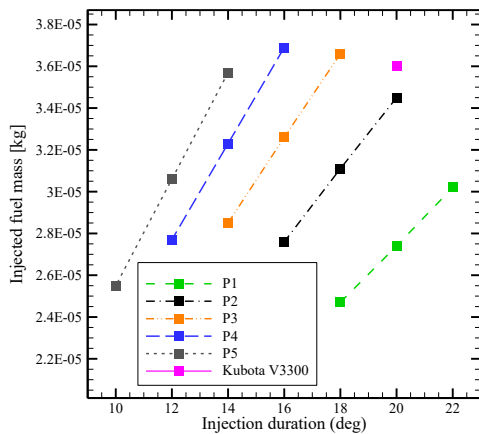


**Fig. 7.** Variations of the fuel inlet mass for different injection pressures and duration.

Comparison of all cases obtained from the 5 injection pressures, each having 3 injection durations, causes the resulting diagrams to be crowded and so confusing. Therefore, for the sake of brevity, two injection pressures (P2 and P5) were selected on behalf of the other

pressures, and effect of injection pressure and duration was investigated (pressure P1 was not selected due to the production of less power than the Kubota engine). Fig. 8 shows the effect of different injection pressure and durations on the pressure inside the combustion chamber. Also, Fig. 9 shows combustion chamber temperature in terms of the crankshaft angle (700 to 760 degrees). In case P5, since the fuel is injected in shorter time duration, the peak point of diagram is shifted to earlier crank angles. Moreover, due the higher fuel flow rate, the growth rate of pressure and temperature is higher compared to case P2.

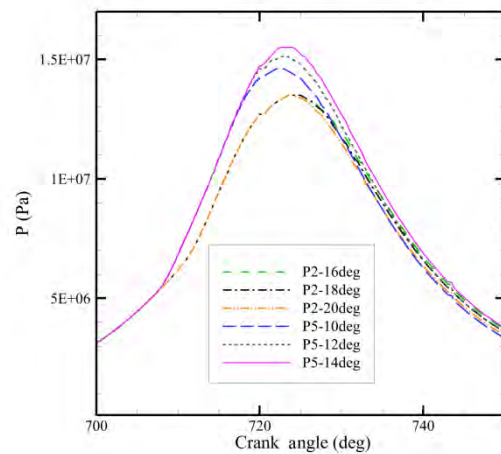


**Fig. 8.** Variations of combustion chamber pressure for different injection cases.

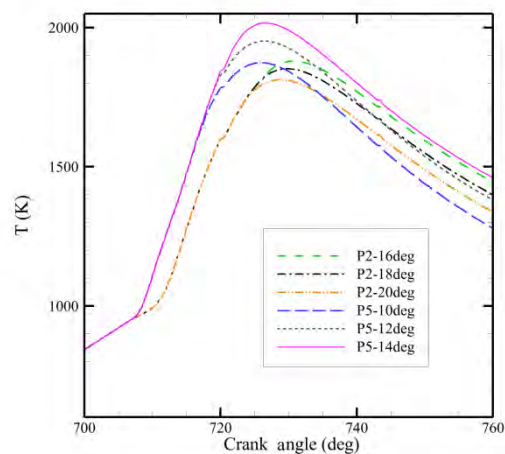


**Fig. 9.** Variations of combustion chamber temperature for different injection cases.

Fig. 10 shows specific fuel consumption (SFC) in an engine operating cycle. For comparison, the experimental results for the Kubota 3300 engine with a conventional injector are presented together with the numerical results for five injection pressures of the annular cross-section injector. Comparing the results for the 5 injection pressures with the results presented for the conventional injector, it is concluded that changing the injector from the conventional mode to the annular cross-section injector, the performance of the Kubota motor is improved. For the cases P1 and P2 and injection durations 20 degrees, compared to the Kubota 3300 engine, SFC is decreased by 15.8% and 13.4%, respectively. The maximum reduction is for case P5 and injection durations 10 degrees, which is decreased by 21.4%. The slope of the SFC curve in all 5 injection pressures is almost the same, so the injection pressure has little effect on fuel atomization in annular cross-section injector. According to Sharma et al. [18], non-circular fuel injectors show better fuel atomization compared to injectors with a circular cross-section orifice, because these types of injectors have better primary fuel droplet breakage compared to conventional injectors due to initial distortions. Among these injectors are the annular injectors studied in the present study. The difference between the present work and the work of Sharma et al. [18] is that they investigated orifice geometries with square, triangular, and rectangular cross-section outlets compared to circular cross-section outlet, while the present study has investigated the orifice geometry with annular cross-section outlet in comparison with the circular cross-section outlet.

SFC is lower in low injection pressures, because more oxygen is available in these conditions. In short injection duration, fuel and air are mixed better, since more time is available for mixing. Also, due to the less fuel mass entering the combustion chamber, there is a higher percentage of air, which improves the quality of fuel and air mixing. Therefore, in all 5 studied cases, the combustion efficiency decreases with the increase in the injection duration, which results in an increase in SFC.

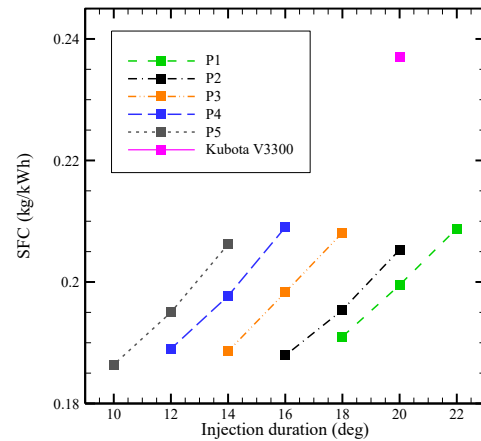


Fig. 10. SFC for different injection cases.

Power produced for different injection pressures (each having three injection durations), as well as the experimental results for the Kubota engine are shown in Fig. 11. Moreover, changes of inlet fuel mass and power for comparing the annular injector with the conventional injector are given in Table 6 for all cases. Comparing the results shows that although the fuel mass has been reduced from the initial 36mg to lower values (Fig. 7 and Table 6), power is almost similar to the results of the Kubota engine. Therefore, using the annular cross-section injector instead of the conventional injector in the Kubota 3300 engine, increases its power, and improves the engine performance. The maximum power increase is 15% for a 2.5% increase in fuel at injection pressure of 100MPa.

The results of Migliaccio et al. [20] also demonstrate that the annular cross-section injectors show better characteristics compared to the conventional circular injectors in the atomization and uniform spraying of fuel due to the increase in the angle of the spray cone and its wide extent. The difference between the present work and the work of Migliaccio et al. [20] is that they only investigated the fuel injection for the annular cross-section outlet, but in addition to their work, the present study has also investigated the combustion of the spray in a diesel engine for different conditions with different injection durations.

At low injection durations, due to the greater reduction in the fuel mass, power is less compared to the Kubota engine. However, even



in these cases, fuel consumption reduction is of greater importance compared to power reduction.

At high injection durations, power is higher than the Kubota engine (except for P1 injection pressure that the amount of fuel input is very low), and although the engine volume is constant, the Kubota engine has been able to produce more power by changing the injector type (the change of fuel amount is shown in Table 6). It is important to note that although the SFC is lower in short injection durations, but due to the more fuel injection in long injection durations and the increase in the input fuel mass, the output power is higher.

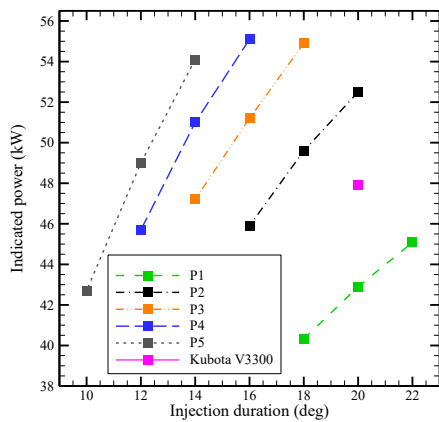


**Fig. 11.** Variations of power with different injection pressures.

At each injection pressure, power decreases as the injection duration reduces, which is due to the fuel mass decrease. Also, Comparison of the 5 injection pressures with each other shows that the factors such as: the inlet mass, volume of the fuel burned before TDC and the improvement of the combustion process have caused difference between the power values of the injection pressures. Power produced up to the injection pressure P3 has an increasing trend, but then decrease (the inlet mass rate had similar trend). Of course, another factor is effective in reducing power; by increasing the injection pressure, the maximum pressure points move away from TDC, which reduces the produced power.

**Table 6.** Variations of inlet fuel mass and power for different cases.

| Case number | Time duration (deg) | Inlet mass changes (%) | Power changes (%) |
|-------------|---------------------|------------------------|-------------------|
| P1          | 22                  | -16.111                | -5.887            |
|             | 20                  | -23.889                | -10.480           |
|             | 18                  | -31.389                | -15.825           |
| P2          | 20                  | -4.167                 | 9.645             |
|             | 18                  | -13.611                | 3.633             |
|             | 16                  | -23.333                | -4.217            |
| P3          | 18                  | 1.667                  | 14.656            |
|             | 16                  | -9.444                 | 6.973             |
|             | 14                  | -20.833                | -1.545            |
| P4          | 16                  | 2.500                  | 14.990            |
|             | 14                  | -10.278                | 6.389             |
|             | 12                  | -23.056                | -4.551            |
| P5          | 14                  | -0.833                 | 12.902            |
|             | 12                  | -15.000                | 2.297             |
|             | 10                  | -29.167                | -10.814           |

Nitrogen oxide production for the two injection pressures P2 and P5 is demonstrated in Fig. 12. At the onset of combustion, temperature inside the combustion chamber rises, leading to increases in the produced NO amount. The amount of this pollutant reaches a constant value a few degrees aTDC, because all the fuel burns, and the high temperature points disappear. Also, after TDC, the combustion chamber begins to expand, which results in a decrease in temperature. Also, during the expansion stroke, the mixing process is faster and better, which leads to the mixing of high temperature and low temperature areas in the combustion chamber.

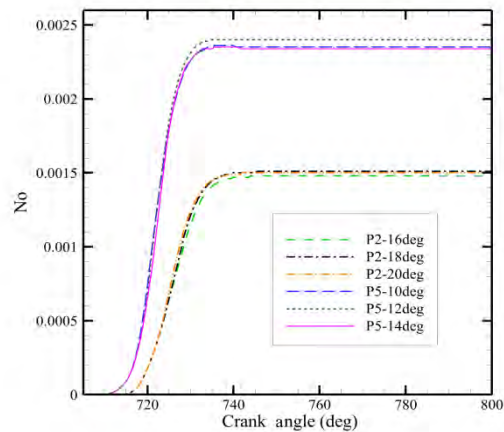


**Fig. 12.** NO variations for different cases.

Comparing the amount NO at pressures P2 and P5, it can be observed that the produced NO in the P5 pressure is higher due to the entry of more fuel in the initial degrees of injection, leading to higher pressure and temperature. Comparing both injection pressures with the base case (conventional circular injector), it can be concluded that the use of annular injector in the Kubota 3300 engine has increased NO production. This is due to the fact that by improving the combustion performance of the engine using the annular cross-section injector, the temperature and pressure of the combustion chamber have increased, causing more nitrogen decomposition in the combustion chamber. Therefore, by reducing the injection pressure and controlling the fuel inlet, it is possible to prevent the temperature of the combustion chamber from increasing too much, which results in decrease of NO production.

Fig. 13 shows the mass fraction of soot in terms of crankshaft angle. It is observed that with the onset of combustion and increase of chamber temperature due to the speed of reactions and lack of proper oxygen supply to the combustion fuel, amount of the soot increases. After the end of the main combustion due to deceleration of chemical reactions and appropriate temperature and intensity of the turbulence created inside the cylinder, the soot created is oxidized and reduced to an appropriate amount.

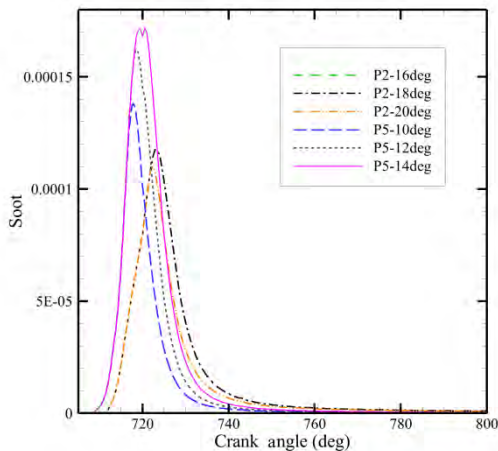


Fig. 13. Soot variations for different cases.

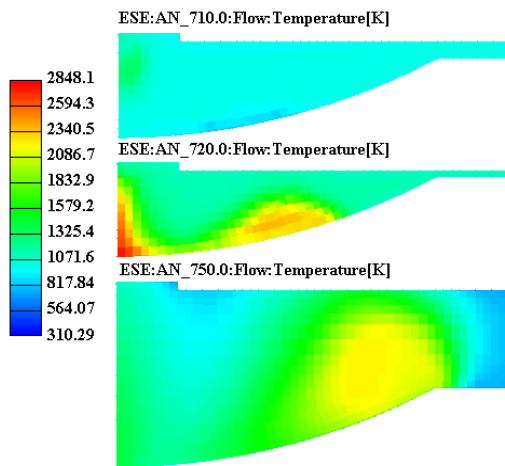
The first increase is due to premixed combustion: when premixed combustion

occurs, the oxygen around the flame decreases sharply. However, as the flame progresses inside the chamber after TDC, soot oxidation begins and carbon particles are combined with oxygen, which is then supplied to the molecules, and get consumed. In all cases, the soot is well oxidized and eliminated at the end, and the engine has no problem producing soot. Therefore, application of the annular injector in the Kubota 3300 engine causes no problems in terms of soot pollution.

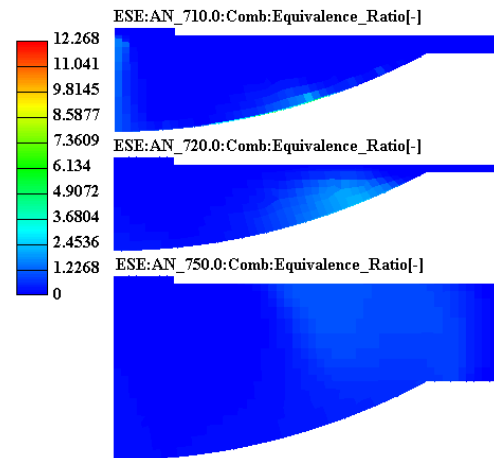
Fig. 14 shows the temperature distribution and how the flame front moves. As can be seen, the combustion starts from the central zone and gradually moves towards the cylinder walls. At first, the movement towards the walls is high, which decreases with the expansion of the combustion chamber. At 120MPa injection pressure, the temperature rise is greater compared to 40MPa injection pressure, because the fuel injection flow rate is higher at this pressure and more energy is released before TDC. As demonstrated in Fig. 15, combustion occurs in areas with equivalence ratio greater than 2.

Considering soot and NO distribution contours, it is observed that both pollutants are produced more at high temperature points. As demonstrated in Fig. 16, NO is formed in the poorer region of the high temperature zone, while soot is formed in the richer region of the high temperature zone. In regions with an equivalence ratio of 1 and temperature above 2000K, nitrogen oxide has the highest concentration. Since the combustion chamber temperature increase for the 120MPa injection pressure is greater compared to the 40MPa injection pressure, the NO production is higher for it.

Fig. 17 shows the soot distribution. Soot is produced in the flame front and in oxygen-poor regions, where the rate of oxygen penetration into the combustion zone is not sufficient to reach stoichiometric conditions, which are mostly near the piston crown. By comparing the soot distribution at the two angles of TDC and 30° aTDC, it can be seen that the soot produced at the beginning of combustion is well oxidized and eliminated at the end.

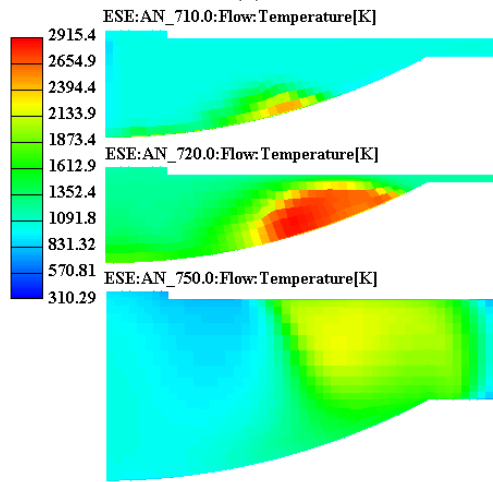


(a)



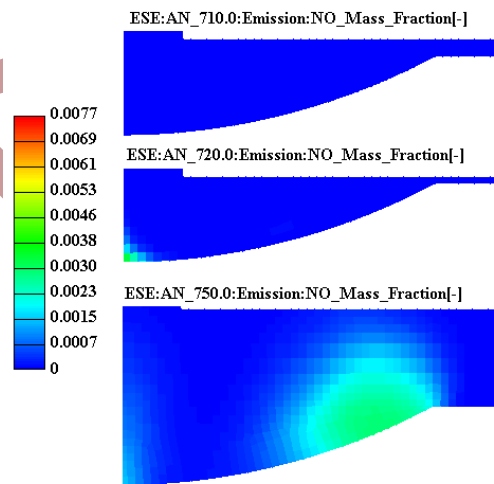
(b)

**Fig. 15.** Distribution of equivalence ratio in the combustion chamber: (a) 40MPa and (b) 120MPa.

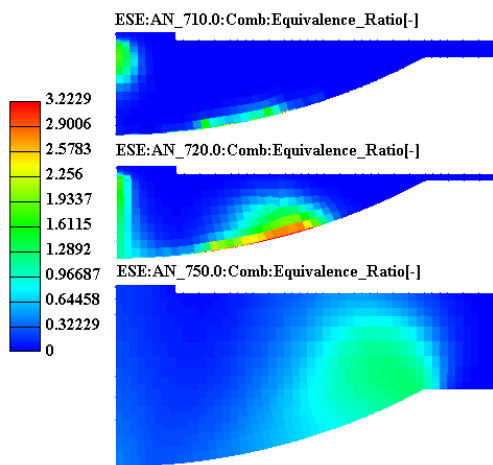


(b)

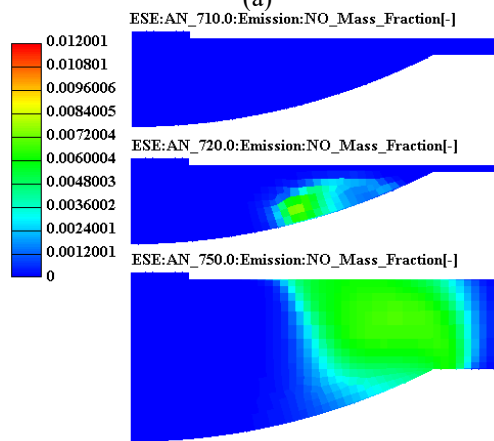
**Fig. 14.** Temperature distribution in the combustion chamber: (a) 40MPa and (b) 120MPa.



(a)



(a)



(b)

**Fig. 16.** Distribution of NO in combustion chamber: (a) 40MPa and (b) 120MPa.

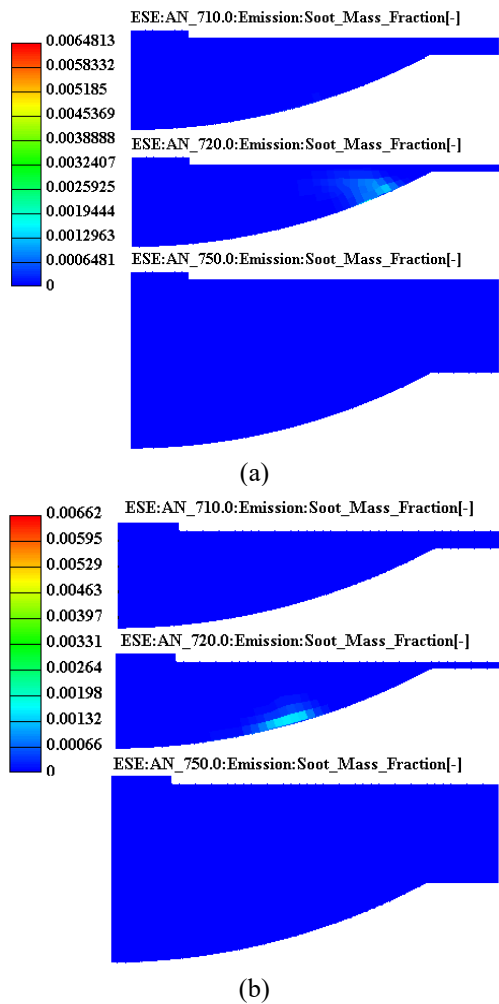


**Fig. 17.** Distribution of soot in the combustion chamber: (a) 40MPa and (b) 120MPa.

Fig. 18 shows how to spray fuel into the combustion chamber 5 and 10° bTDC for pressures 40MPa and 100MPa. The annular cross-section injector increases the angle of the spray cone, which the injector used in the present study, has done well. Considering the distributed droplets, it can be seen that the diameter of the droplets are close to each other, and the droplets are distributed evenly from the central region to the lateral surface of the spray cone.

The formation of this form of fuel spray increases the combustion efficiency for two reasons: Firstly, more fuel evaporates in the pre-combustion stage, and mixes with air, which results in better combustion. Secondly, the homogenous fuel droplets distribution and

increase in the fuel spray angle, increases the flame front surface in the diffusion combustion stage, and air (oxygen) enters the front surface more quickly, which also results in better combustion. Due to the mentioned reasons, the annular injector shows better performance than the conventional injector. The comparison between the pressures of 40 MPa and 100 MPa shows that by increasing the pressure, the diameter of the droplets becomes smaller, and the distribution becomes more uniform. Also, considering that the injection duration is shorter at 100 MPa pressure, so compared to the 40 MPa pressure, the fuel droplets are less seen at the angle of 715 degrees.

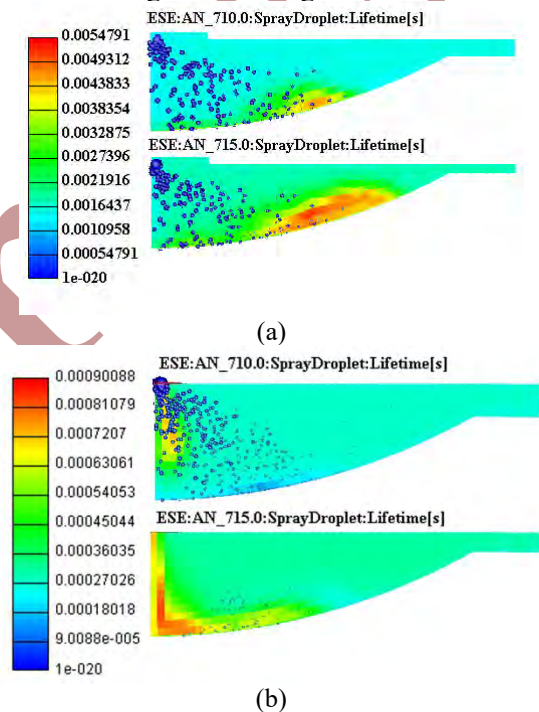


**Fig. 18.** Distribution of the fuel droplets in the combustion chamber: (a) 40MPa and (b) 100MPa.

### 7. Conclusions

In the present study, effects of injection pressure and duration on the performance and emissions characteristics of the Kubota 3300 engine with the new presented annular cross-section injector were investigated numerically. The injection pressure was changed from 40 to 120MPa, while at each pressure three different injection durations were used. In all cases, the start of injection was selected 20° bTDC (as in the Kubota 3300 engine). Effects of injection



pressure and duration on power, specific fuel consumption and emissions were investigated for all cases. A summary of the important results of the study is as follows:

- Although in most cases the fuel inlet mass is less compared to the engine with conventional injector, the produced power is higher compared to the engine with conventional circular injector. The more uniform distribution of fuel in the annular injector improves the fuel and air mixing, and increases the combustion efficiency. This leads to an increase in the produced power in the case with the annular injector compared to the combustion chamber with a conventional injector. The maximum power increase was 15% for a 2.5% increase in fuel at injection pressure of 100MPa.
- At most cases, although power is increased, the SFC value was lower compared to the engine with the conventional injector. This is caused by the more homogenous distribution of the fuel air mixture. The maximum reduction in SFC value is for case P5 and injection durations 10 degrees, which is decreased by 21.4%.
- Increasing the injection pressure improved the fuel distribution in the combustion chamber, but due to the tendency of the maximum pressure and temperature distribution to earlier angles bTDC, effect of the mentioned proper distribution on enhancing engine performance was slightly reduced.
- Nitrogen oxide (NO) production was higher compared to the engine using the conventional injector due to the enhanced power and higher temperature and pressure in the combustion chamber.

## References

- [1] F. El-Mahallawy, S.D. Habik, *Fundamentals and technology of combustion*, Elsevier, (2002).
- [2] J.B. Heywood, *Internal combustion engine fundamentals*, McGraw-Hill Education, (2018).
- [3] Y. Zhang, K. Nishida, S. Nomura, T. Ito, Spray characteristics of group-hole nozzle for DI diesel engine, 0148-7191, *SAE technical paper*, (2003).
- [4] J. Gao, Y. Matsumoto, M. Namba, K. Nishida, "An investigation of mixture formation and in-cylinder combustion processes in direct injection diesel engines using group-hole nozzles", *Int. J. Engine Res.*, Vol. 10, No. 1, pp. 27-44, (2009).
- [5] S.W. Park, R.D. Reitz, "Optimization of fuel/air mixture formation for stoichiometric diesel combustion using a 2-spray-angle group-hole nozzle", *Fuel*, Vol. 88, No. 5, pp. 843-852, (2009).
- [6] S.W. Park, H.K. Suh, C.S. Lee, N. Abani, R.D. Reitz, "Modeling of group-hole-nozzle sprays using grid-size-, hole-location-, and time-step-independent models", *Atomization Sprays*, Vol. 19, No. 6, pp. (2009).
- [7] D. Siebers, B. Higgins, "Flame lift-off on direct-injection diesel sprays under quiescent conditions", *SAE Transactions*, pp. 400-421, (2001).
- [8] K. Nishida, J. Gao, Y. Matsumoto, "Experimental study on spray and mixture properties of the group-hole nozzle for direct-injection diesel engines, Part II: effects of included angle and interval between orifices", *Atomization Sprays*, Vol. 19, No. 4, pp. (2009).
- [9] A. Pawlowski, R. Kneer, A.M. Lippert, S.E. Parrish, "Investigation of the interaction of sprays from clustered orifices under ambient conditions relevant for diesel engines", *SAE Int. J. Engines*, Vol. 1, No. 1, pp. 514-527, (2009).
- [10] X. Wang, Z. Huang, W. Zhang, O.A. Kuti, K. Nishida, "Effects of ultra-high injection pressure and micro-hole nozzle on flame structure and soot formation of impinging diesel spray", *Appl. Energy*, Vol. 88, No. 5, pp. 1620-1628, (2011).
- [11] D. Montgomery, M. Chan, C. Chang, P. Farrell, R.D. Reitz, Effect of injector nozzle hole size and number on spray characteristics and the performance of a heavy duty DI diesel engine, 0148-7191, *SAE Technical Paper*, (1996).

- [12] P. Bergstrand, M. Försth, I. Denbratt, "The influence of orifice diameter on flame lift-off length", *Zaragoza*, Vol. 9, No., pp. 11, (2002).
- [13] C. Sayin, M. Gumus, M. Canakci, "Influence of injector hole number on the performance and emissions of a DI diesel engine fueled with biodiesel–diesel fuel blends", *Appl. Therm. Eng.*, Vol. 61, No. 2, pp. 121-128, (2013).
- [14] S.J.M. Algayyim, A.P. Wandel, T. Yusaf, "The impact of injector hole diameter on spray behaviour for butanol-diesel blends", *Energies*, Vol. 11, No. 5, pp. 1298, (2018).
- [15] M. Vijay Kumar, A. Veeresh Babu, P. Ravi Kumar, T. Manoj Kumar Dundi, "Influence of different nozzle hole orifice diameter on performance, combustion and emissions in a diesel engine", *Aust. J. Mech. Eng.*, Vol. 18, No. 2, pp. 179-184, (2020).
- [16] L.G. Dodge, T.W. Ryan III, M.G. Ryan, "Effects of different injector hole shapes on diesel sprays", *SAE transactions*, pp. 1160-1168, (1992).
- [17] P. Sharma, T. Fang, "Spray and atomization of a common rail fuel injector with non-circular orifices", *Fuel*, Vol. 153, pp. 416-430, (2015).
- [18] P. Sharma, T. Fang, "Breakup of liquid jets from non-circular orifices", *Exp. Fluids*, Vol. 55, pp. 1-17, (2014).
- [19] K. Sakaki, T. Funahashi, S. Nakaya, M. Tsue, R. Kanai, K. Suzuki, T. Inagawa, T. Hiraiwa, "Longitudinal combustion instability of a pintle injector for a liquid rocket engine combustor", *Combust. Flame*, Vol. 194, pp. 115-127, (2018).
- [20] M. Migliaccio, A. Montanaro, C. Beatrice, P. Napolitano, L. Allocca, V. Fraioli, "Experimental and numerical analysis of a high-pressure outwardly opening hollow cone spray injector for automotive engines", *Fuel*, Vol. 196, pp. 508-519, (2017).
- [21] H. Gao, F. Zhang, Z. Zhang, E. Wang, B. Liu, "Experimental investigation on the spray characteristic of air-assisted hollow-cone gasoline injector", *Appl. Therm. Eng.*, Vol. 151, pp. 354-363, (2019).
- [22] L. Wang, F. Wang, T. Fang, "Flash boiling hollow cone spray from a GDI injector under different conditions", *Int. J. Multiphase Flow*, Vol. 118, No., pp. 50-63, (2019).
- [23] H. Wu, F. Zhang, Z. Zhang, H. Gao, "Experimental investigation on the spray characteristics of a self-pressurized hollow cone injector", *Fuel*, Vol. 272, pp. 117710, (2020).
- [24] M.T. Shervani-Tabar, R. Esmaelnadjad, S.E. Razavi, M. Jafari, "Study on the effects of the injection pressure of an annulus nozzle and combustion chamber on the performance of a diesel engine", *J. Mech. Eng.*, Vol. 49, No. 4, pp. 125-134, (2019).
- [25] S.W. Park, H.J. Kim, C.S. Lee, Investigation of atomization characteristics and prediction accuracy of hybrid models for high-speed diesel fuel sprays, 0148-7191, *SAE Technical Paper*, (2003).
- [26] R. Payri, J.P. Viera, H. Wang, L.-M. Malbec, "Velocity field analysis of the high density, high pressure diesel spray", *Int. J. Multiphase Flow*, Vol. 80, pp. 69-78, (2016).
- [27] C.S. Lee, S.W. Park, "An experimental and numerical study on fuel atomization characteristics of high-pressure diesel injection sprays", *Fuel*, Vol. 81, No. 18, pp. 2417-2423, (2002).
- [28] J. Cha, S.Y. Yang, N. Naser, A.I. Ichim, S.H. Chung, High pressure and split injection strategies for fuel efficiency and emissions in DI diesel engine, 0148-7191, *SAE Technical Paper*, (2015).
- [29] M.G. Shatrov, L.N. Golubkov, A.U. Dunin, A.L. Yakovenko, P.V. Dushkin, "Influence of high injection pressure on fuel injection performances and diesel engine working process", *Therm. Sci.*, Vol. 19, No. 6, pp. 2245-2253, (2015).
- [30] P. Carlucci, A. Ficarella, D. Laforgia, "Effects of pilot injection parameters on combustion for common rail diesel engines", *SAE Trans.*, pp. 932-943, (2003).
- [31] B. Jayashankara, V. Ganesan, "Effect of fuel injection timing and intake pressure on the performance of a DI diesel engine—A

- parametric study using CFD", *Energy Convers. Manage.*, Vol. 51, No. 10, pp. 1835-1848, (2010).
- [32] L.-M. Malbec, W.E. Eagle, M.P. Musculus, P. Schihl, "Influence of injection duration and ambient temperature on the ignition delay in a 2.34 L optical diesel engine", *SAE Int. J. Engines*, Vol. 9, No. 1, pp. 47-70, (2016).
- [33] C. Zhang, A. Zhou, Y. Shen, Y. Li, Q. Shi, "Effects of combustion duration characteristic on the brake thermal efficiency and NOx emission of a turbocharged diesel engine fueled with diesel-LNG dual-fuel", *Appl. Therm. Eng.*, Vol. 127, pp. 312-318, (2017).
- [34] A.H. Lefebvre, V.G. McDonell, *Atomization and sprays*, CRC press, (2017).
- [35] C. Clark, N. Dombrowski, "Aerodynamic instability and disintegration of inviscid liquid sheets", *Proceedings of the Royal Society of London. A. Math. and Phys. Sci.*, Vol. 329, No. 1579, pp. 467-478, (1972).
- [36] A. Brink, C. Mueller, P.A. KILPINEN, M. Hupa, "Possibilities and limitations of the eddy break-up model", *Combust. Flame*, Vol. 123, No. 1-2, pp. 275-279, (2000).
- [37] K. Nishida, H. Hiroyasu, "Simplified three-dimensional modeling of mixture formation and combustion in a DI diesel engine", *SAE Trans.*, pp. 276-293, (1989).
- [38] J.K. Dukowicz, "A particle-fluid numerical model for liquid sprays", *J. Comput. Phys.*, Vol. 35, No. 2, pp. 229-253, (1980).
- [39] N. Hassan, M. Rasul, C.A. Harch, "Modelling and experimental investigation of engine performance and emissions fuelled with biodiesel produced from Australian Beauty Leaf Tree", *Fuel*, Vol. 150, pp. 625-635, (2015).